

Electronic Supplementary Information

Band Gap and Magnetism Engineering of Penta-Graphene via Adsorption of Small Transition Metal Clusters

Jia Chen^a, Hong Cui^{b,c,*}, Peng Wang^a, Yanfei Zheng^a, Dandan Wang^a, Hong Chen^a, Hongkuan Yuan^{a,*}

^a School of Physical Science and Technology, Southwest University, Chongqing, 400715, China

^b Shaanxi Key Laboratory of Industrial Automation, Shaanxi University of Technology, Hanzhong, Shaanxi, 723001, China

^c School of Mechanical Engineering, Shaanxi University of Technology, Hanzhong, Shaanxi, 723001, China

* Corresponding authors:

E-mail: hongcui@snut.edu.cn; yhk10@swu.edu.cn

Contents:

Table S1-6: The detail results of TM adatoms and clusters at the bridge site on PG sheet, including formation energy E_{f0} (in eV), adsorption energy E_{ad} (in eV), averaged C₁-C₁ bond-length l_{C1-C1} between the nearest C₁ atoms that adjoint TM atom, TM-C₁ bond-length l and l' between TM atom and its nearest C₁ atoms, vertical height d , spin magnetic moment μ under the scalar-relativistic calculations. Spin μ_s and orbital μ_l magnetic moment as well as magnetic anisotropy energy MAE (in meV) under the spin-orbital coupling calculations with in-plane (x axis) and out-of-plane (z axis) magnetizations, respectively. The lengths are in angstrom (in Å) and magnetic moments are in Bohr magneton (in μ_B). Tables S1-5 are for TM adatom at bridge-site and top-site configurations, dimers in D1 and D2 configurations, TM₄ and TM₅ clusters in M4 and M5 configurations, respectively.

Table S7: Comparisons of adsorption energy, structure parameters and spin magnetic moment between the calculations without (PBE) and with non-bonded intramolecular dispersion corrections (PBE+D3).

Figure S1: Top-views of nine distinctive adsorption sites of singlet atom adsorption.

Figure S2: The adsorption sites of TM₂ dimer, and the relative stability of these adsorptions for Co₂ dimer.

Figure S3: The same as Figure S2, but for clusters $n=3-5$.

Figure S4: Adsorption height d and formation energy E_{f0} of TM₄ tetramer in M4-configuration (up-panel) and pentamer in M5-configuration (down-panel). Insert charts are for average TM-TM bond-lengths.

Figure S5 : AIMD results for total energy and simulation temperatures of Co_n clusters on 4×4 PG sheet. Inset charts are side-view and top-view snapshots of atomic configuration at the end of simulation.

Figure S6: Band structures of singlet atom adsorption (B, T configurations). Solid black and red lines represent the majority and minority spin channels, respectively. The Fermi level is set to zero. The CBM and VBM are characterized by the black points at the high-symmetry points in the irreducible wedges of the Brillouin zone.

Figure S7: Same as in Fig. S6, but for TM_2 dimer adsorption (D1, D2 configurations).

Figure S8: Same as in Fig. S6, but for tetramer TM_4 and TM_5 pentamer adsorption (M4 and M5 configurations).

Figure S9 : Band structures (a) and DOS (b, c) of pristine PG sheet. Black and green lines represent the band structures with HSE and PBE calculations; Purple and blue line represent the projected DOS on C_1 atoms (b) and C_2 atoms (c) with HSE calculation. The Fermi level is set to zero.

Figure S10: Band structures of Fe@PG system with the bridge-site deposition configuration (a-b) and top-site deposition configuration (c-d). Black and red lines represent spin-up and spin-down states, respectively; PBE bands are shown in (a) and (c) panel while HSE bands are shown in (b) and (d) panel, respectively; band-gap E_g of spin-up, spin-down and total band are shown.

Figure S11: Orbital magnetic moments in parallel and perpendicular magnetization (μ_B), and the MAEs (meV).

Table S1: The detail results of TM adatoms at the bridge site on PG sheet, including formation energy E_{fo} (in eV), adsorption energy E_{ad} (in eV), averaged C₁-C₁ bond-length $l_{C_1-C_1}$ between the nearest C₁ atoms that adjoint TM atom, TM-C₁ bond-length l and l' between TM atom and its nearest C₁ atoms, vertical hight d , spin magnetic moment μ under the scalar-relativistic calculations. Spin μ_s and orbital μ_l magnetic moment as well as magnetic anisotropy energy MAE (in meV) under the spin-orbital coupling calculations with in-plane (x axis) and out-of-plane (z axis) magnetizations, respectively. The lengths are in angstrom (in Å) and magnetic moments are in Bohr magneton (in μ_B).

Adatom	E_{fo}	E_{ad}	$l_{C_1-C_1}$	l_1	l'_1	d	μ	In-plane (x)		Out-plane (z)		MAE
								$\vec{\mu}_s$	$\vec{\mu}_l$	$\vec{\mu}_s$	$\vec{\mu}_l$	
Fe@PG _b	2.29	2.29	1.47	1.88	1.88	1.86	2.02	2.02	0.05	2.02	0.15	0.82
Co@PG _b	2.67	2.67	1.44	1.89	1.89	1.86	0.99	0.98	0.03	0.99	0.32	2.61
Ru@PG _b	3.28	3.28	1.46	2.00	2.00	1.99	1.68	1.67	0.05	1.68	0.52	10.06
Rh@PG _b	3.39	3.39	1.44	2.01	2.01	1.98	0.78	0.74	0.04	0.77	0.22	0.31
Os@PG _b	3.10	3.10	1.48	1.97	1.97	1.96	1.61	1.50	0.11	1.63	1.10	113.24
Ir@PG _b	3.74	3.74	1.46	2.00	2.00	1.99	0.90	0.10	-0.02	0.92	1.60	21.15

Table S2: Same as in Table 1, but for TM adatoms at top-site on PG substrate.

Adatom	E_{fo}	E_{ad}	$l_{C_1-C_1}$	l_1	l'_1	d	μ	In-plane (x)		Out-plane (z)		MAE
								$\vec{\mu}_s$	$\vec{\mu}_l$	$\vec{\mu}_s$	$\vec{\mu}_l$	
Fe@PG _t	2.03	2.03	1.41	1.94	1.94	1.39	2.18	2.17	0.09	2.17	0.10	0.97
Co@PG _t	2.62	2.62	1.40	1.91	1.91	1.33	1.13	1.11	0.13	1.11	0.13	0.70
Ru@PG _t	3.00	3.00	1.40	2.05	2.05	1.52	1.81	1.79	0.18	1.79	0.24	1.29
Rh@PG _t	3.09	3.09	1.40	2.00	2.11	1.50	0.82	0.81	0.18	0.80	0.08	0.31
Os@PG _t	2.82	2.82	1.40	1.95	1.99	1.19	1.63	1.46	0.24	1.47	0.40	10.03
Ir@PG _t	3.80	3.80	1.38	1.95	2.04	1.20	0.72	0.66	0.20	0.67	0.28	1.91

Table S3: Same as in Table 1, but for TM dimers on PG sheet with D1-configuration. Dimer bond-length is represented by a , and magnetic moment is averaged over each atom.

Adatom	E_{fo}	E_{ad}	$l_{C_1-C_1}$	a	l_1	l'_1	d	$\bar{\mu}$	In-plane (x)		Out-plane (z)		MAE
									$\vec{\mu}_s$	$\vec{\mu}_l$	$\vec{\mu}_s$	$\vec{\mu}_l$	
Fe ₂ @PG _{D1}	2.96	1.60	1.42	2.23	1.94	2.19	1.87	2.68	2.68	0.05	2.68	0.08	-0.01
Co ₂ @PG _{D1}	3.16	1.59	1.42	2.19	1.90	2.13	1.81	1.23	1.23	0.14	1.22	0.17	0.33
Ru ₂ @PG _{D1}	4.25	2.18	1.44	2.27	2.00	2.18	1.91	0.87	0.87	0.07	0.87	0.13	1.12
Rh ₂ @PG _{D1}	3.88	2.32	1.43	2.52	1.99	2.15	1.94	-0.032	0.03	0.01	-0.03	0.05	0.25
Os ₂ @PG _{D1}	4.74	2.35	1.46	2.27	1.99	2.17	1.90	0.83	0.83	0.03	0.78	0.25	-1.79
Ir ₂ @PG _{D1}	4.70	2.34	1.45	2.40	1.97	2.12	1.88	0.83	0.36	0.15	0.34	0.14	-0.68

Table S4: Same as in Table 1, but for TM dimers on PG sheet with D2-configuration.

Adatom	E_{fo}	E_{ad}	$l_{C_1-C_1}$	a	l_1	l'_1	d	$\bar{\mu}$	In-plane (x)		Out-plane (z)		MAE
									$\vec{\mu}_s$	$\vec{\mu}_l$	$\vec{\mu}_s$	$\vec{\mu}_l$	
Fe ₂ @PG _{D2}	3.12	1.73	1.45	2.21	1.97	1.96	1.43	2.04	2.04	0.06	2.04	0.05	0.24
Co ₂ @PG _{D2}	3.27	1.74	1.43	2.23	1.94	1.99	1.41	1.10	1.10	0.12	1.10	0.08	-0.84
Ru ₂ @PG _{D2}	4.25	2.29	1.47	2.36	1.99	2.12	1.63	1.65	1.65	0.13	1.64	0.06	-0.82
Rh ₂ @PG _{D2}	3.74	2.19	1.43	2.23	1.98	2.11	1.41	0.76	0.76	0.2	0.74	0.05	-2.82
Os ₂ @PG _{D2}	4.54	2.28	1.46	2.39	2.00	2.12	1.41	0.70	0.19	0.18	0.06	0.06	-4.12
Ir ₂ @PG _{D2}	4.38	2.09	1.47	2.45	1.99	2.12	1.63	0.87	0.75	0.31	0.71	0.18	-8.34

Table S5: Same as in Table 1, but for TM₄ clusters on PG sheet with M4-configuration.

Adatom	E_{fo}	E_{ad}	$l_{C_1-C_1}$	a	l_1	l'_1	d	$\bar{\mu}$	In-plane (x)		Out-plane (z)		MAE
									$\vec{\mu}_s$	$\vec{\mu}_l$	$\vec{\mu}_s$	$\vec{\mu}_l$	
Fe ₄ @PG _{M4}	3.52	1.25	1.43	2.33	2.00	2.01	1.87	2.39	2.39	0.06	2.39	0.07	0.32
Co ₄ @PG _{M4}	3.75	1.28	1.41	2.28	1.94	2.00	1.81	1.50	1.49	0.14	1.49	0.12	-0.23
Ru ₄ @PG _{M4}	4.71	1.46	1.42	2.38	1.99	2.12	1.88	0.33	0.21	0.00	0.21	-0.01	0.36
Rh ₄ @PG _{M4}	4.42	1.73	1.41	2.51	1.98	2.11	1.85	0.80	0.79	0.08	0.76	0.07	-2.17
Os ₄ @PG _{M4}	5.79	1.87	1.43	2.37	2.00	2.12	1.87	0.00	0.00	0.00	0.00	0.00	0.00
Ir ₄ @PG _{M4}	5.56	1.81	1.42	2.42	1.99	2.12	1.89	0.41	0.33	0.07	0.36	0.12	3.63

Table S6: Same as in Table 1, but for TM₅ clusters on PG sheet with M5-configuration.

Adatom	E_{fo}	E_{ad}	$l_{C_1-C_1}$	a	l_1	l'_1	d	$\bar{\mu}$	In-plane (x)		Out-plane (z)		MAE
									$\bar{\mu}_s$	$\bar{\mu}_l$	$\bar{\mu}_s$	$\bar{\mu}_l$	
Fe ₅ @PG _{M5}	3.54	0.90	1.43	2.40	1.94	2.06	1.82	2.40	2.40	0.07	2.40	0.07	-0.12
Co ₅ @PG _{M5}	3.95	1.17	1.41	2.36	1.88	2.04	1.75	1.45	1.45	0.14	1.45	0.11	-0.64
Ru ₅ @PG _{M5}	5.07	1.57	1.41	2.44	2.01	2.16	1.91	0.38	0.38	0.06	0.38	0.04	-0.02
Rh ₅ @PG _{M5}	4.54	1.44	1.40	2.54	1.99	2.16	1.91	0.89	0.53	0.04	0.53	0.08	0.71
Os ₅ @PG _{M5}	5.93	1.74	1.43	2.45	2.00	2.14	1.88	0.37	0.37	0.14	0.36	0.07	-3.14
Ir ₅ @PG _{M5}	5.77	1.82	1.42	2.51	2.00	2.13	1.89	0.50	0.42	0.11	0.34	0.08	-17.30

Table S7: Comparisons of adsorption energy, structure parameters and spin magnetic moment between the calculations without (PBE) and with non-bonded intramolecular dispersion corrections (PBE+D3).

Systems	E_{ad}		l_1		l'_1		$l_{C_1-C_1}$		d		μ	
	PBE	PBE+D3	PBE	PBE+D3	PBE	PBE+D3	PBE	PBE+D3	PBE	PBE+D3	PBE	PBE+D3
Fe ₁ @PG _b	2.29	2.49	1.88	1.88	1.89	1.89	1.47	1.46	1.86	1.86	2.02	2.03
Fe ₁ @PG _t	2.03	2.22	1.94	1.94	1.94	1.94	1.41	1.41	1.39	1.39	2.18	2.10
Fe ₂ @PG _{D1}	1.60	1.81	1.94	2.19	1.90	2.16	1.42	1.44	1.87	1.82	2.68	2.31
Fe ₂ @PG _{D2}	1.73	1.93	1.97	1.96	1.97	1.97	1.45	1.44	1.43	1.44	2.04	2.30
Co ₁ @PG _b	2.67	2.87	1.89	1.89	1.89	1.89	1.44	1.44	1.86	1.86	0.99	1.00
Co ₁ @PG _t	2.62	2.80	1.91	1.91	1.90	1.90	1.40	1.40	1.33	1.32	1.11	1.13
Co ₂ @PG _{D1}	1.59	1.78	1.90	2.13	1.90	2.09	1.42	1.43	1.81	1.77	1.23	1.20
Co ₂ @PG _{D2}	1.74	1.98	1.94	1.99	1.92	1.99	1.43	1.42	1.41	1.41	1.10	1.10

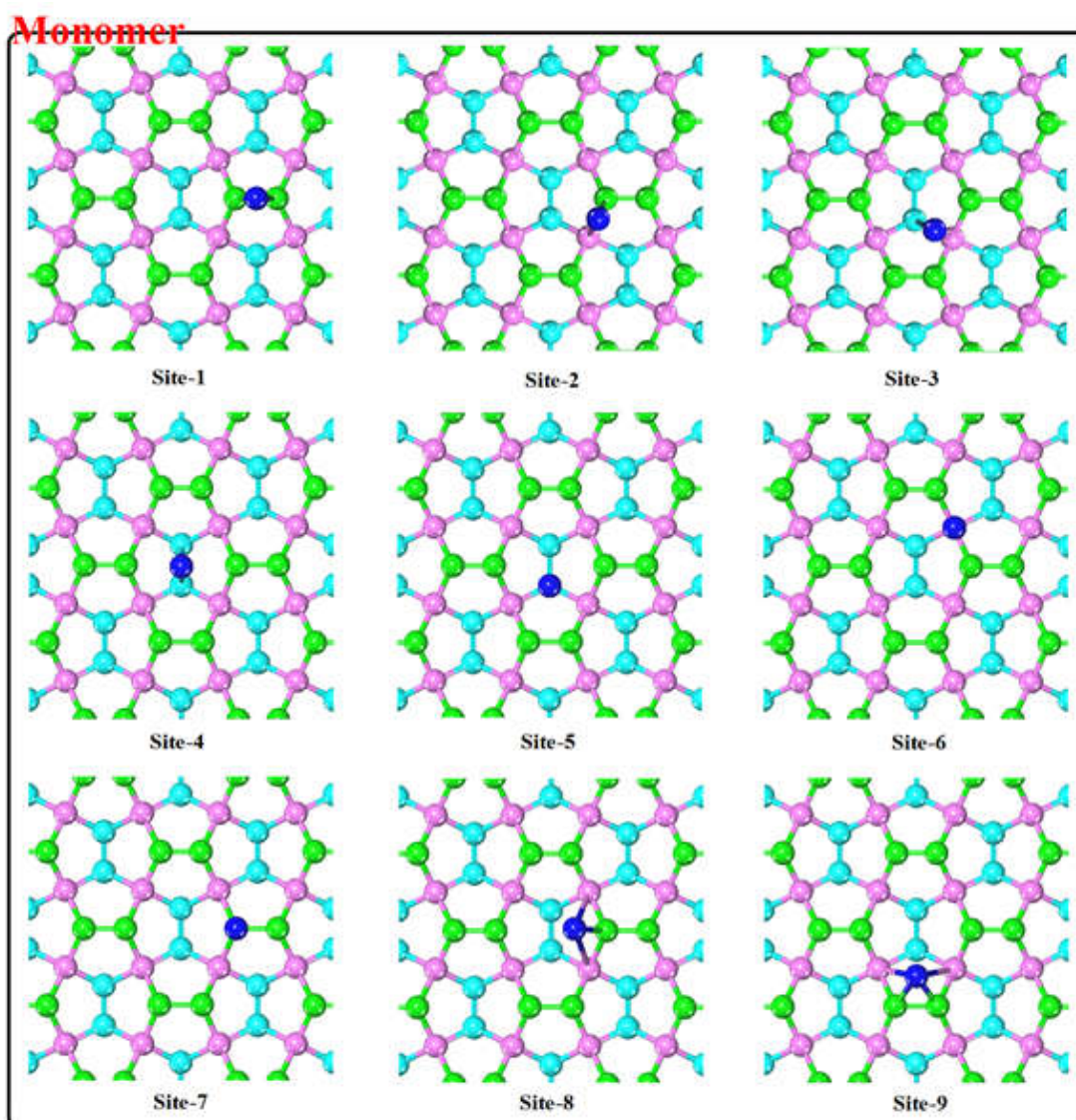


Figure S1: Top views of nine distinctive adsorption sites of singlet atom adsorption.

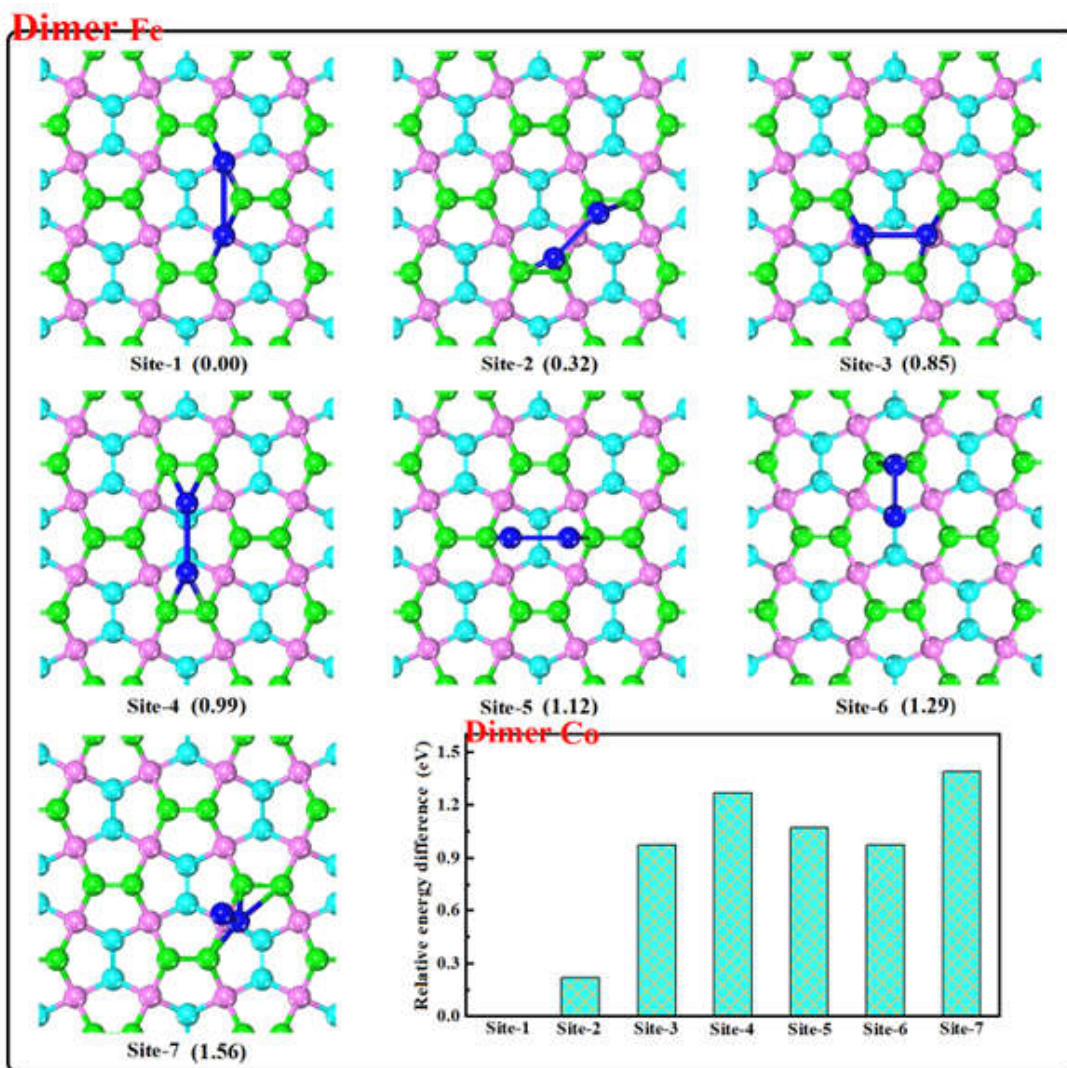


Figure S2: The adsorption sites of TM_2 dimer, and the relative stability of these adsorptions for Fe_2 and Co_2 dimers are in eV.

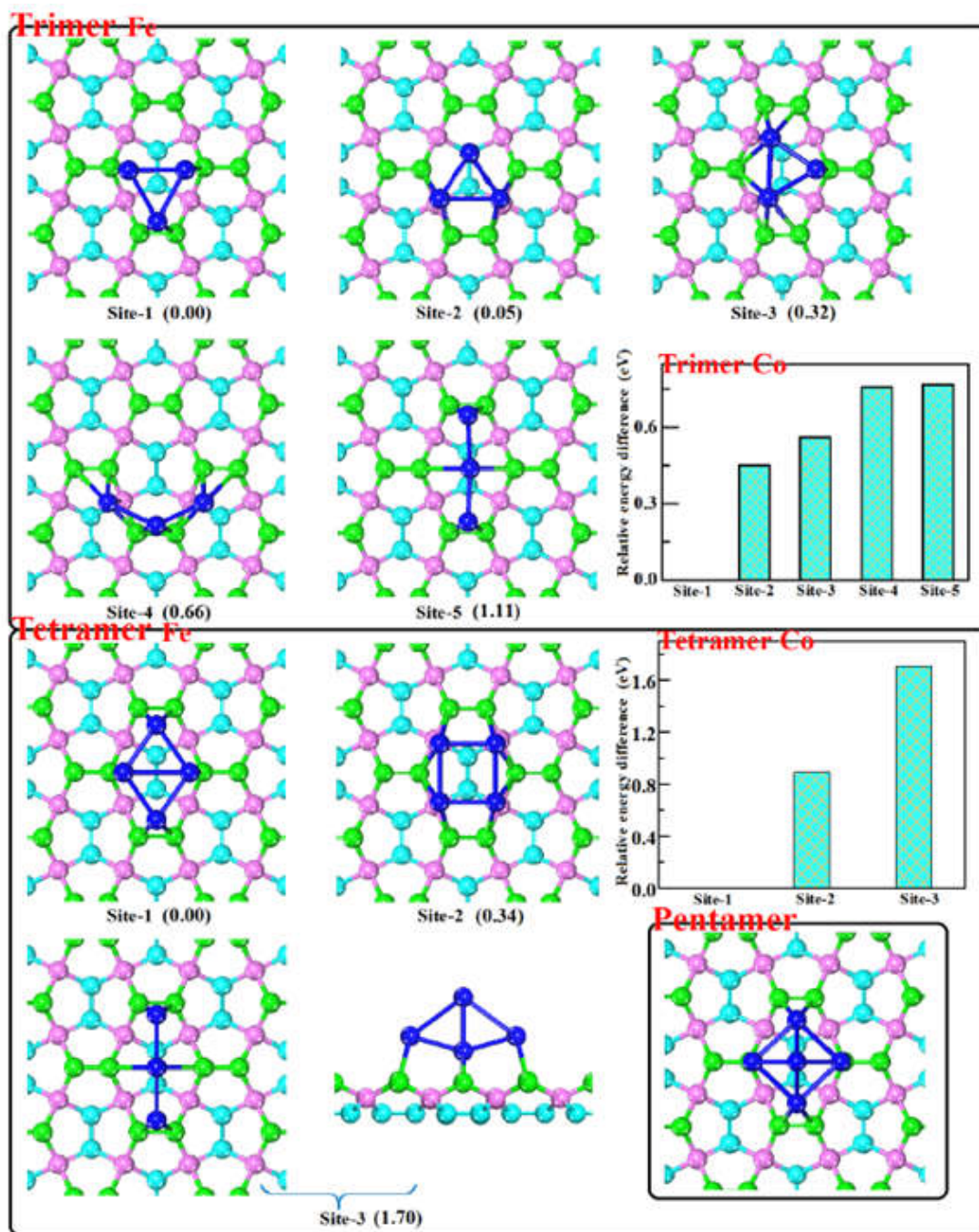


Figure S3: The same as Figure S2, but for clusters $n=3-5$.

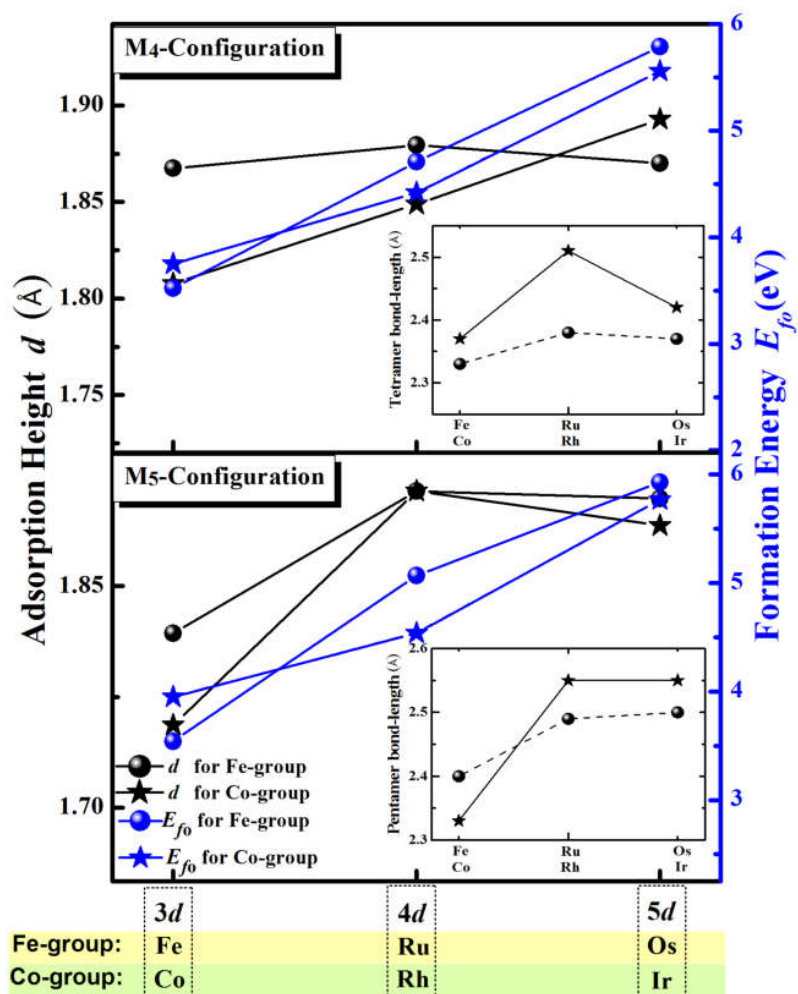


Figure S4: Adsorption height d and formation energy E_{fo} of TM₄ tetramer in M4-configuration (up-panel) and pentamer in M5-configuration (down-panel). Insert charts are for average TM-TM bond-lengths.

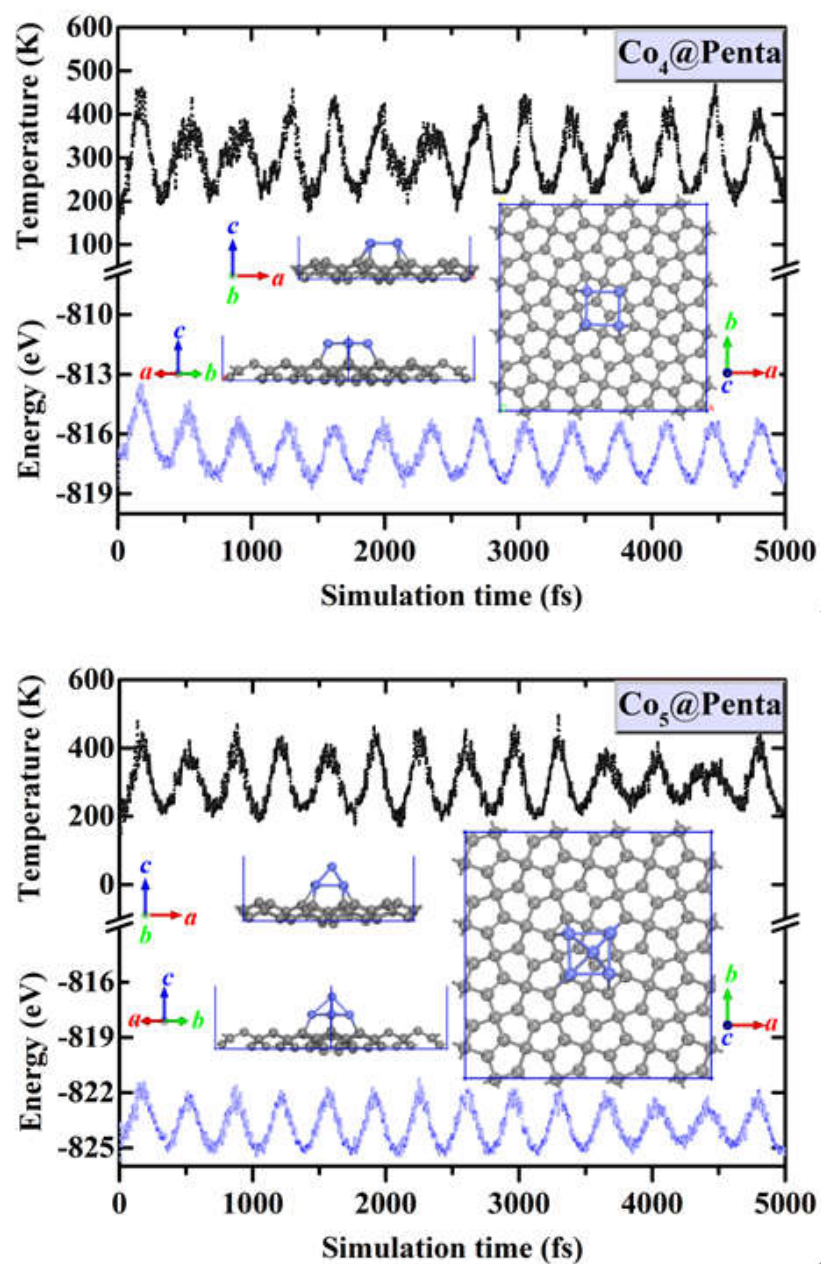


Figure S5 : AIMD results for total energy and simulation temperatures of Co_n clusters on 4×4 PG sheet. Inset charts are side-view and top-view snapshots of atomic configuration at the end of simulation.

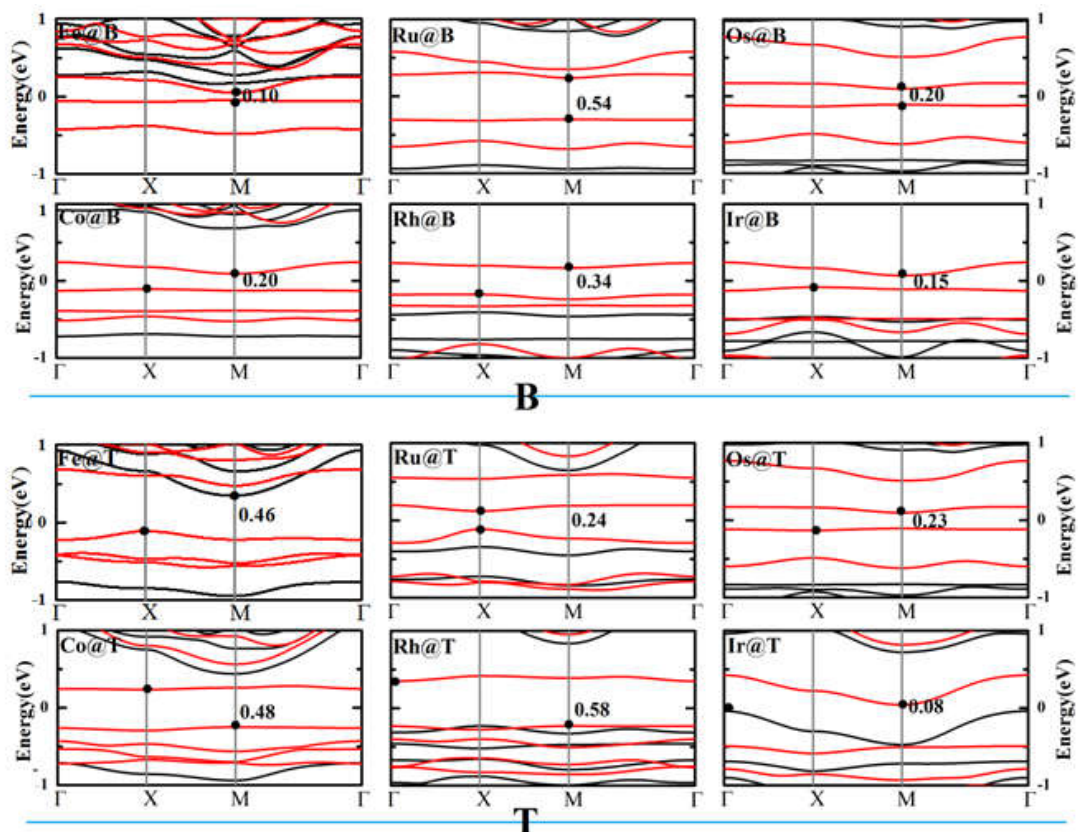


Figure S6: Band structures of singlet atom adsorption (B, T configurations). Solid black and red lines represent the majority and minority spin channels, respectively. The Fermi level is set to zero. The CBM and VBM are characterized by the black points at the high-symmetry points in the irreducible wedges of the Brillouin zone.

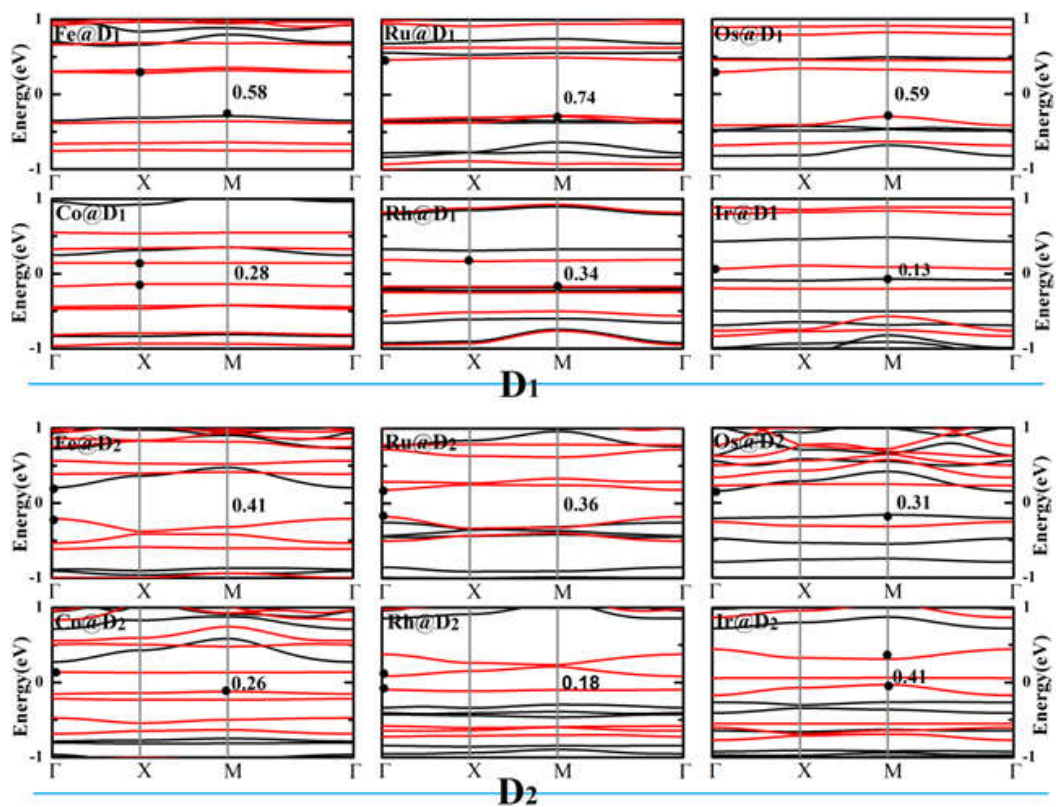


Figure S7: Same as in Fig. S6, but for TM_2 dimer adsorption (D1, D2 configurations).

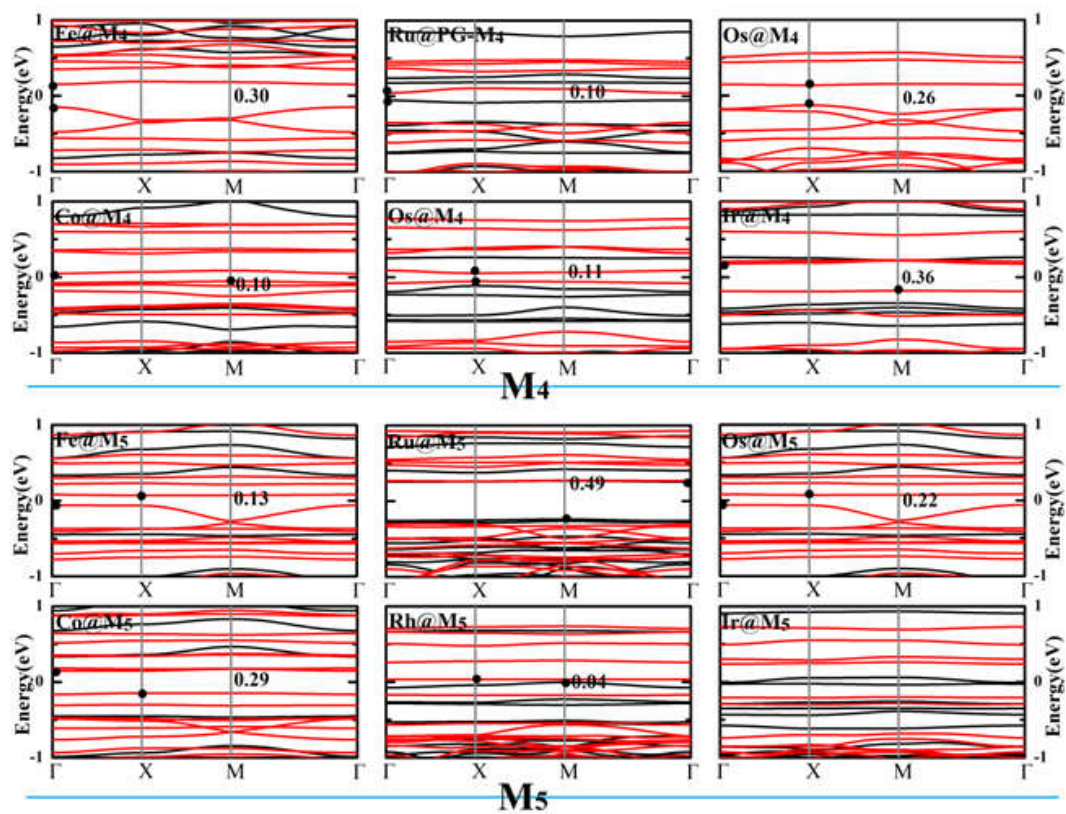


Figure S8: Same as in Fig. S6, but for TM₄ and TM₅ clusters adsorptions (in M₄ and M₅ configurations).

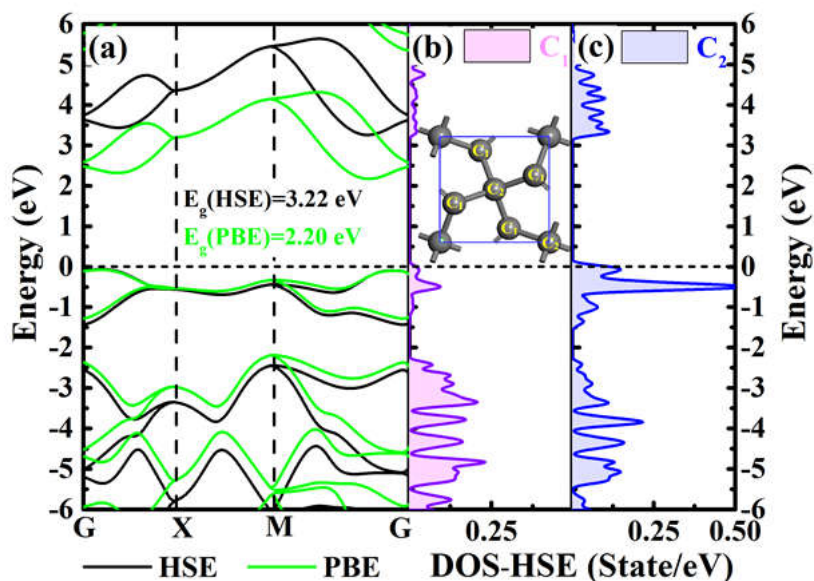


Figure S9 : Band structures (a) and DOS (b, c) of pristine PG sheet. Black and green lines represent the band structures with HSE and PBE calculations; Purple and blue line represent the projected DOS on C_1 atoms (b) and C_2 atoms (c) with HSE calculation. The Fermi level is set to zero.

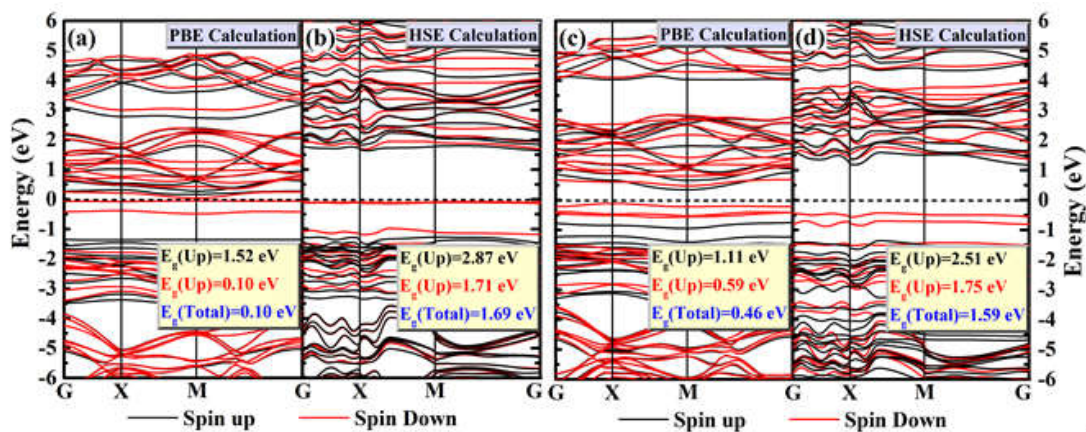


Figure S10: Band structures of Fe@PG system with the bridge-site deposition configuration (a-b) and top-site deposition configuration (c-d). Black and red lines represent spin-up and spin-down states, respectively; PBE bands are shown in (a) and (c) panel while HSE bands are shown in (b) and (d) panel, respectively; band-gap E_g of spin-up, spin-down and total band are shown.

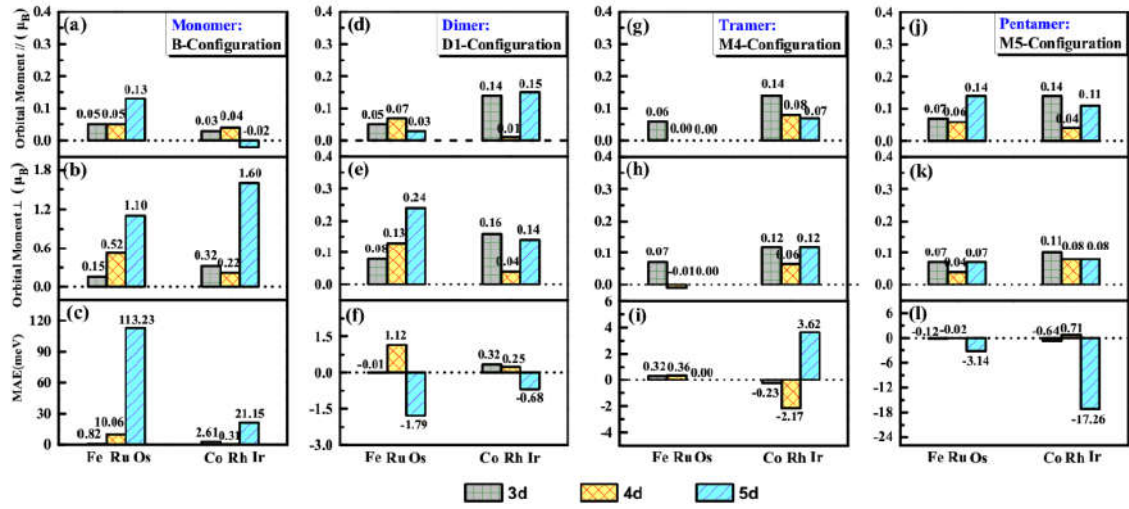


Figure S11 : Orbital magnetic moments in parallel and perpendicular magnetization (μ_B), and the MAEs (meV).